Plant Physiol. (1995) 109: 1317–1326

Electrochemical Potential Gradients of H^+, K^+, Ca^{2+}, and Cl^- across the Tonoplast of the Green Alga *Eremosphaera viridis*[1]

Birgit Bethmann, Manfred Thaler, Wilhelm Simonis, and Gerald Schönknecht*

Julius-von-Sachs-Institut für Biowissenschaften der Universität Würzburg, Lehrstuhl Botanik I, Mittlerer Dallenbergweg 64, 97082 Würzburg, Germany

Using ion-selective microelectrodes, we measured the activity of H^+, K^+, Ca^{2+}, and Cl^- and the electrical potential both in the vacuole and in the cytoplasm of the unicellular green alga *Eremosphaera viridis* to obtain comparable values of the named parameters from the same object under identical conditions. The cytosol had a pH of 7.3, and activities of the other ions were 130 mM K^+, 160 nM Ca^{2+}, and 2.2 mM Cl^-. We observed only small and transient light-dependent changes of the cytosolic Ca^{2+} activity. The vacuolar K^+ activity did not differ significantly from the cytosolic one. The Ca^{2+} activity inside the vacuole was approximately 200 μM, the pH was 5.0, and the Cl^- activity was 6.2 mM. The concentrations of K^+, Ca^{2+}, and Cl^- in cell extracts were measured by induction-coupled plasma spectroscopy and anion chromatography. This confirmed the vacuolar activities for K^+ and Cl^- obtained with ion-selective microelectrodes and indicated that approximately 60% of the vacuolar Ca^{2+} was buffered. The tonoplast potential was vanishingly low (≤±2 mV). There was no detectable electrochemical potential gradient for K^+ across the tonoplast, but there was, however, an obvious electrochemical potential gradient for Cl^- (−26 mV), indicating an active accumulation of Cl^- inside the vacuole.

Vacuoles play a central role in the physiology of plants. Some of their most important functions include storage of anions, Ca^{2+}-regulation, turgor regulation, and detoxification. All of these tasks are accomplished by specific transport proteins in the tonoplast. To understand the physiological role of these transport systems it is essential to know the ion activity gradients and the electrical potential difference across the tonoplast inside an intact plant cell (Martinoia 1992; Taiz, 1992; Tyerman, 1992). Energization of the vacuole is provided by two H^+-translocating pumps generating a transmembrane pH gradient and an electric potential positive inside the vacuole (Rea and Sanders, 1987). The H^+ gradient is used for the uptake of organic and inorganic substances into the vacuole. The accumulation of Ca^{2+} inside the vacuole is probably accomplished by a Ca^{2+}/H^+ antiporter (Schumaker and Sze, 1985; Evans et al., 1991), although recent results propose the existence of a Ca^{2+}-ATPase in the tonoplast (Gavin et al., 1993; Pfeiffer and Hager, 1993). There is increasing evidence that Ca^{2+} release from the vacuole is involved in Ca^{2+} signaling (Schumaker and Sze, 1987a; Evans et al., 1991; Bush, 1993), and an inositol 1,4,5-trisphosphate-activated Ca^{2+} channel was discovered in the tonoplast (Alexandre et al., 1990). To understand the mechanisms of Ca^{2+} accumulation and Ca^{2+} release it is necessary to know the proportion of bound Ca^{2+} to free Ca^{2+}. Most of the vacuolar Ca^{2+} is probably buffered by organic acids or calcium-binding proteins (Randall, 1992). The K^+ concentration inside the vacuole seems to be comparable to the cytosol or less, depending on the growth conditions (Flowers and Läuchli, 1983; Leigh and Win Jones, 1984; Maathuis and Sanders, 1993). Little is known about the transporters that could maintain a K^+ gradient across the tonoplast.

There seems to be general agreement about the accumulation of anions inside the vacuole by the electrical potential difference across the tonoplast (Blumwald and Poole, 1985; Hedrich et al., 1988; Martinoia, 1992; Taiz, 1992). This assumption is based on tonoplast potentials of −20 mV and larger (sign convention as proposed in Bertl et al., 1992; extracytosolic space is treated as the reference point). However, data in the literature concerning tonoplast potentials vary, and lower values are frequently reported (summarized by Gibrat et al., 1985). Very little is known about anion activities in plant cells (Tyerman, 1992), and a direct relationship between the anion gradient (e.g. for Cl^-) and the tonoplast potential has not yet been proved. It is not known how the magnitude of the tonoplast potential is regulated or how the balance between pH gradient and tonoplast potential, both generated by the H^+-pumps, is achieved. To answer these questions, it is important to know the activities of the different ions on both sides of the membrane as well as the membrane potential. Ion-selective microelectrodes provide an excellent technique for measuring the ion activity and the electrical potential of a certain compartment directly and synchronously.

In the present study, the activity of H^+, K^+, Ca^{2+}, and Cl^- and the electrical potential was measured with ion-selective microelectrodes in the vacuole as well as in the cytoplasm. In addition, the concentrations of K^+, Ca^{2+}, and Cl^- were measured in the cell sap. On the basis of these

[1] This work was supported by the Deutsche Forschungsgemeinschaft (SFB 176, TP B11).

* Corresponding author; e-mail gerald@botanik.uni-wuerzburg.de; fax 49-931-888-6158.

Abbreviations: ICP, induction-coupled plasma spectroscopy; {ion}, activity of the ion.

data we calculated the degree of Ca^{2+} binding inside the vacuole and the driving forces for all four ions across the tonoplast.

MATERIALS AND METHODS

Plant Material

The coccal green alga *Eremosphaera viridis* de Bary (algal culture collection, Göttingen, Germany) was cultivated as described by Köhler et al. (1983). The culture had an average density of 11,000 cells/mL and a cell cycle of 5 to 7 d. All experiments were performed in artificial pond water, containing 0.1 mM KNO_3, 0.1 mM $MgCl_2$, 0.2 mM $CaCl_2$, and 2 mM Mes, and the pH was adjusted to pH 5.6 with NaOH. For impalements, algae with diameters of at least 150 μm were selected (full-grown cells without indications of cleavage), with a spherical shape and a dark green color.

Experimental Setup

Algal cells were fixed by a suction pipette in a perfusion chamber and impaled with the help of mechanical micromanipulators. Illumination was provided by a cold light source equipped with light-conducting fiber (KL1500; Schott, Mainz, Germany). Experiments were performed with photosynthetically saturating white light of 500 μmol m^{-2} s^{-1} at a temperature of 20 ± 2°C. Intracellular ion activities were measured with ion-selective microelectrodes (Ammann, 1986). Because ion-selective microelectrodes respond to the ion activity as well as to the electrical potential of their environment, a synchronous measurement of the electrical potential has to be performed. This was carried out using a separate voltage electrode or, alternatively, a θ-shaped double-barreled glass capillary containing both electrodes. Non-turgor-resistant ion-selective microelectrodes were used. Impalements were made possible by turgor reduction, which, as in preceding studies (Thaler et al., 1992; Trebacz et al., 1994), was achieved by the addition of 400 mM sorbitol to the artificial pond water. Electrode potentials were measured by a high-input impedance amplifier (Frankenberger, Germering, Germany) and registered by a pen recorder (model 314; Kontron, Munich, Germany). Calibration of the ion-selective electrode was performed before and after each measurement. Ion activity calculations were based on the second calibration data because small changes in electrode characteristics could be attributed to the impalement. The resistance of the ion-selective electrode was routinely checked during the experiment to ensure the integrity of the sensor. All membrane potentials are related to a reference point outside the cytosol (Bertl et al., 1992). Specifically, the potential difference across the tonoplast was calculated as the cytosolic electrical potential minus the vacuolar electrical potential.

Electrode Characteristics

Borosilicate glass capillaries with inner filaments (Hilgenberg, Malsfeld, Germany) were used for single-barreled microelectrodes and potential electrodes. The potential electrode was filled with 0.5 M KCl to keep tip potentials low while preventing leakage of the electrolyte into the cells. For Cl^- measurements only 0.1 mM KCl was used to minimize Cl^- leakage. The preparation of ion-selective electrodes has been described in detail elsewhere (Trebacz et al., 1994). In short, a silanization procedure in a hot oven was used, and the electrodes were filled from the back side. Double-barreled electrodes were fabricated from θ-shaped glass capillaries with thick septum (World Precision Instruments, Sarasota, FL; TST 150–6). Before silanization the blunt end of the future potential electrode was closed by a drop of glue. The capillary was placed on a hot plate at 420°C, and the silanization agent, *N,N*-dimethyltrimethylsilylamine (Fluka), was injected into the open shank. The potential electrode was filled either with 0.5 M KCl for pH electrodes or with 1 M sodium acetate plus 10 mM NaCl for K^+ electrodes. The future ion-selective electrode was first backfilled with electrolyte, and application of pressure resulted in the filling of the tip region. A small drop of sensor was then placed into the electrolyte at a position near the tip of the electrode. The sensor moved into the tip by itself because of hydrophobic forces. All sensors are commercially available from Fluka: hydrogen ionophore II-cocktail A, Fluka No. 95297; potassium ionophore I-cocktail B, Fluka No. 60398; calcium ionophore II-cocktail A, Fluka No. 21196; chloride ionophore I-cocktail A, Fluka No. 24902.

Electrolytes for the ion-selective electrodes were 40 mM KH_2PO_4, 23 mM NaOH, 15 mM NaCl (pH 7) for pH electrodes; the calibration solution for a concentration of 100 mM K^+ for K^+ electrodes; 0.1 μM Ca^{2+} for Ca^{2+} electrodes, and 100 mM Cl^- for Cl^- electrodes. Calibrations were performed in the following solutions: pH electrodes: pH 5, pH 7, and pH 8 in an ionic background of 100 mM KCl and 30 mM NaCl; K^+ electrodes: 50 mM, 100 mM, 200 mM, and 500 mM KCl with an ionic background of 10 mM NaCl adjusted to pH 7.4 by 5 mM Tris/HCl; Ca^{2+} electrodes: solutions with concentrations ranging from 10 nM to 1 mM (Fig. 1) according to Ammann et al. (1987); Cl^- electrodes: 1, 3, 10, and 100 mM KCl. Ionic strength was kept constant by the addition of 99, 97, 90, and 0 mM K^+ gluconate buffered to pH 7.4 by 10 mM Tris/H_2SO_4. Ion activities of K^+ and Cl^- solutions were calculated by a Debye-Hückel formalism; parameters were taken from Meier et al. (1980). According to Tsien and Rink (1980), activity coefficients in the Ca^{2+} calibration solutions were assumed to be 1. Electrodes were characterized by the voltage change induced by a 10-fold increase in activity (slope). A decrease of sensitivity of ion-selective electrodes was observed for low activities of Ca^{2+} and Cl^-. In these cases calibration values were fitted by the Nicolsky-Eisenman equation. Electrodes were additionally characterized by their limit of detection, which represents the ion activity for which the calibration curve has a half-maximum slope (International Union of Pure and Applied Chemistry, 1976). Single-barreled pH electrodes had a slope of 54 ± 3 mV (n = 60); θ-shaped pH electrodes had practically the same slope of 51 ± 3 mV (n = 65). Single-barreled K^+ electrodes had a slope of 56 ± 2 mV (n = 21); θ-shaped K^+ electrodes had almost the same slope of 51 ± 3 mV (n = 16). K^+ and pH electrodes

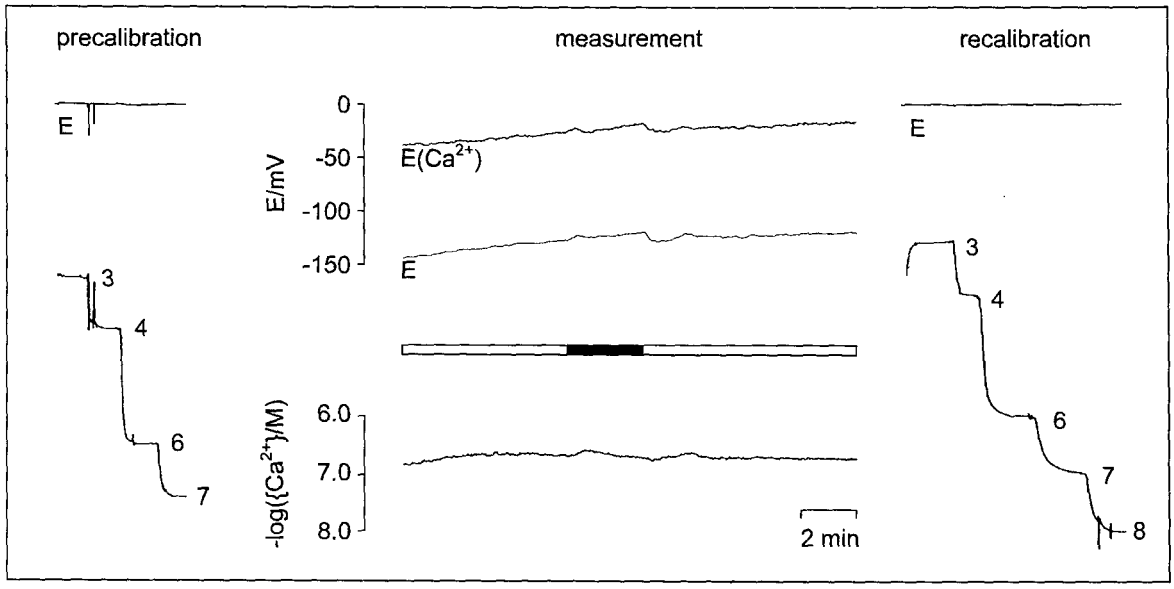

Figure 1. Precalibration (left), measurement (middle), and recalibration (right) of a Ca^{2+}-selective microelectrode. The original trace of the potential recorded by the Ca^{2+}-selective microelectrode [E(Ca^{2+})] was omitted for the calibrations for clarity. Only the recording of the membrane potential (E) electrode and the difference between the two electrodes giving the logarithmic Ca^{2+} activity are shown for the calibration. During the measurement (middle) with both electrodes inserted into *E. viridis*, the Ca^{2+}-selective microelectrode recorded the Ca^{2+} activity plus the electrical potential [E(Ca^{2+}), upper trace] and the membrane potential electrode recorded the electrical potential (middle trace). The difference between the two recordings (lower trace, vertically expanded by a factor of 2) gives the logarithm of the cytosolic Ca^{2+} activity. The actual Ca^{2+} activity was calculated from the calibration of the Ca^{2+} electrode after the experiment (right). The Ca^{2+}-selective microelectrode used here had a limit of detection below 10 nM. Small but significant light-dependent changes in the cytosolic Ca^{2+} activity were detected (the bar describes the light protocol).

responded to a 10-fold concentration change within 3 s (90% of voltage change). This time was probably limited by the exchange of the solution. The slope of single-barreled Ca^{2+} electrodes was 28 ± 1 mV (n = 23). Depending on the tip diameter the limit of detection varied from 10 to 260 nM. Higher detection limits were observed for electrodes with smaller tip diameters. Impalement was easier with these electrodes. Although they were insufficient to determine cytosolic Ca^{2+} activities, they could, however, be used for vacuolar measurements. Electrodes with larger tip diameters that had detection limits of 10 to 50 nM were used to measure cytosolic Ca^{2+} activities (Fig. 1). These electrodes were harder to insert into the cell and they never impaled the vacuole. Cl^- electrodes had a slope of −56 ± 4 mV (n = 30) and a limit of detection between 0.1 and 2 mM, depending on the tip diameter. Ca^{2+} and Cl^- electrodes responded to a 10-fold concentration change within 10 to 20 s (90% of voltage change).

Results are stated as means ± SE. The y axis values in the figures giving the logarithmic ion activities directly reflect the calibration performed after the measurement. For measurements with ion-selective electrodes SES are given only for the logarithms of activities because these are distributed in a Gaussian manner (Fry et al., 1990), and for the ion activities mean values only are given.

Cell Sap Measurements

For analysis of cell sap composition, cells were thoroughly washed in distilled water. They were then allowed to settle by gravity, and 1 mL samples of this dense cell suspension were taken. Cells were heated to 100°C for 10 min and centrifuged at 5000 rpm for a further 10 min. The supernatant was analyzed by ICP (JY70PLUS, Instruments SA, Longjumeau, France) and anion chromatography (Schröppel-Meier and Kaiser, 1988). Additional samples were dried overnight at 100°C and then broken down by nitric acid for analysis by ICP. Cell volume was estimated as follows. A nonpermeable coloring (India ink) was added to a dense cell suspension that was diluted with a certain volume by distilled water. The initial and final concentrations of the India ink were determined spectrophotometrically. Cell volume could then be calculated from the known added volume of distilled water and the concentration ratio of the coloring. The dry weight of 1 mL of the dense cell suspension was 42.9 ± 0.8 mg (n = 7) and the cell volume was 0.483 ± 0.016 mL (n = 4).

RESULTS

Measurements with pH-Selective Electrodes

The pH measurements were accomplished with both θ-shaped, double-barreled microelectrodes and two separate microelectrodes, a potential electrode and a pH sensitive one. With double-barreled microelectrodes the potential and the ion activity (plus electrical potential) were measured at exactly the same place. The tips of two different microelectrodes might be in different compartments,

the cytoplasm or the vacuole, and the potentials of these two compartments differ by the tonoplast potential.

pH Values

Recorded pH values stabilized within a few minutes after inserting a pH-sensitive microelectrode into an algal cell. The measured pH values showed two distinct distributions, one at approximately pH 7.3 and the other at approximately pH 5.0 (Fig. 2). We never observed stable pH values in the range between pH 5.2 and 6.7. Thus, the pH electrode was either placed in the vacuole recording a value of approximately pH 5.0 or located in the cytosol, which had a pH of approximately 7.3. The pH values measured with double-barreled and with two separate microelectrodes were identical, pH 7.29 ± 0.03 (n = 64) and 7.28 ± 0.03 (n = 54) for the cytoplasm and pH 5.03 ± 0.08 (n = 9) and 4.99 ± 0.05 (n = 11) for the vacuole, respectively. About 50% of the vacuolar pH recordings were only stable for a few minutes, after which the pH increased and finally stabilized at about pH 7.3; pH changes in the opposite direction never occurred. This was observed for double-barreled (Fig. 2) and single-barreled microelectrodes, with pH shifts from pH 4.95 ± 0.11 to pH 7.29 ± 0.08 (n = 5) and from pH 4.95 ± 0.06 to pH 7.17 ± 0.12 (n = 4), respectively. We interpreted the pH shift as the tip of the electrode being covered by cytoplasm. This process took 1 to 4 min.

In some experiments the reaction to light intensity changes was examined. In the cytoplasm (at pH 7.3) a strong and transient acidification was observed after darkening of the cells, and illumination resulted in a transient alkalization. Very small light-dependent pH changes (0.02 ± 0.01, n = 4) in the same direction were observed inside the vacuole (at pH 5.0).

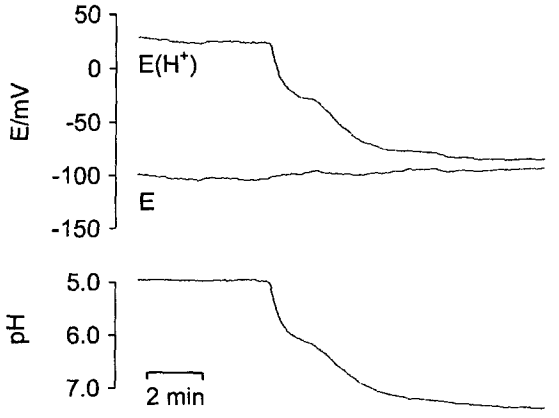

Figure 2. Transmembrane potential (E, middle trace) and intracellular pH (bottom trace) in the unicellular green alga *E. viridis*. The measurement was carried out using a θ-shaped, double-barreled, pH-selective microelectrode. The upper trace shows the original recording of the pH barrel [E(H^+)]. The intracellular pH (bottom trace) results from the difference between the upper two traces. The pH scale was calculated from the calibration of the pH electrode after the experiment. For the first few minutes the pH value was stable but it then shifted to higher values. During this shift the membrane potential (E) was constant.

Electrical Potentials

After impalement with the potential electrode, a hyperpolarization of −160 to −180 mV was observed that came close to the Nernst potential of K^+. This has been explained by the activation of a Ca^{2+}-dependent K^+ conductance and a transient increase in Ca^{2+} because of the impalement (Thaler et al., 1989). The membrane potential stabilized after 10 to 15 min. A resting value of −113 ± 1.8 mV (n = 50) was measured with single-potential electrodes. With double-barreled microelectrodes an electrical potential of −109 ± 1.8 mV (n = 64) was recorded in the cytoplasm (at pH 7.3) and a potential of −111 ± 6 mV (n = 9) was recorded inside the vacuole (at pH 5.0). We paid special attention to those measurements with double-barreled microelectrodes for which the electrode tip was excluded from the vacuole (pH shift from 5.0 to 7.3). Since the two electrode tips are adjacent to each other, they had to be excluded from the vacuole at the same time (Fig. 2). Recorded potentials before and after the transition did not differ significantly from each other (2 ± 2 mV, n = 5). All of these observations indicate a vanishingly small electrical potential difference across the tonoplast of *E. viridis*.

Potassium Measurements

Potassium measurements were performed with θ-shaped, double-barreled microelectrodes and with two separate, single-barreled microelectrodes. The recorded K^+ activity stabilized 1 to 2 min after impalement, which was slightly faster than for the pH recordings. Measurements with double-barreled electrodes yielded an activity of 132 mM ($-\log\{K^+\}$ = 0.880 ± 0.012; n = 11), and two separate electrodes gave an average activity of 130 mM ($-\log\{K^+\}$ = 0.886 ± 0.010; n = 22). Comparable to the pH measurements double-barreled and single-barreled microelectrodes reported exactly the same values. The distribution of the measured activities was investigated in more detail on a logarithmic scale (Fig. 3). The distribution was satisfactorily described by a single Gaussian and a second peak could not be detected. We never observed changes between two different stable values, although they frequently occurred during measurements for all other ions. Light intensity changes did not result in any perceptible change in the K^+ activity.

Calcium Measurements

In our case, pH and K^+ measurements had shown that single-barreled and double-barreled ion-selective microelectrodes resulted in exactly the same activities. On this basis, Ca^{2+} measurements were performed with two separate electrodes for the following reasons. (a) The fabrication of double-barreled microelectrodes is difficult and involves a number of additional problems (Felle, 1988, 1989). (b) With single-barreled electrodes it is possible to vary the tip diameter of the ion-selective microelectrode without changing the potential-measuring electrode (Miller and Sanders, 1987). This was especially important in the case of Ca^{2+}-selective microelectrodes. Ca^{2+} electrodes with smaller tip diameters (pulled as potential elec-

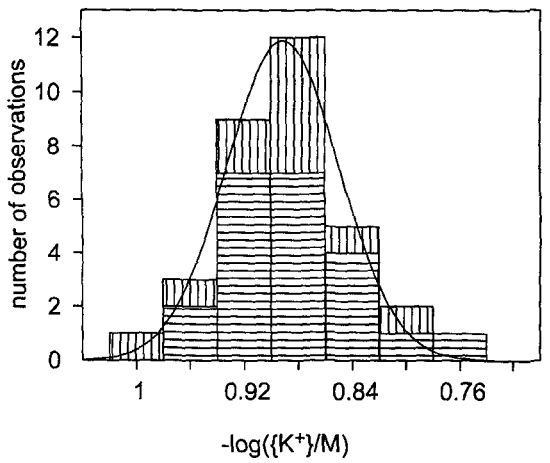

Figure 3. Histogram of the recorded intracellular K^+ activities. The distribution is shown for the negative logarithm of the K^+ activities. The lower horizontally striped rectangles represent measurements with two separate electrodes. The upper vertically striped rectangles represent measurements with θ-shaped, double-barreled microelectrodes. The distribution was fitted by a Gaussian function (0.891 ± 0.042, mean ± SD; solid line).

trodes) had a significantly reduced slope but were easier to insert into the cell and could impale the vacuole. These Ca^{2+} electrodes were used to measure vacuolar Ca^{2+} activities (Fig. 4). Their limit of detection usually was too high (up to 260 nM) to be able to calculate reliable cytosolic Ca^{2+} activities. Ca^{2+} electrodes with larger tip diameters were harder to insert into the cell and could never be inserted into the vacuole. They displayed a lower limit of detection (below 50 nM) and were used to measure cytosolic Ca^{2+} activities (Fig. 1).

Comparable to the pH experiments, two clearly different distributions of values were recorded for the intracellular Ca^{2+} activity. The lower activity was 164 nM ($-\log\{Ca^{2+}\} = 6.79 \pm 0.03$; $n = 22$). A much higher activity of approximately 200 μM ($-\log\{Ca^{2+}\} = 3.69 \pm 0.06$; $n = 4$) was measured only rarely. Thus, in most cases the Ca^{2+}-selective microelectrode was located in the cytosol, which had a low Ca^{2+} activity of about 164 nM, and was only rarely located inside the vacuole, which had an approximately 1000-fold higher activity. A clear transition from a high to a low Ca^{2+} activity was observed in the time course of one measurement (Fig. 4). In this case, the transition was accompanied by an obvious transient change of the electrical potential, which was also observed in some cases when pH-selective microelectrodes were excluded from the vacuole. This potential transient probably reflects a transient hyperpolarization of the plasmalemma by the opening of Ca^{2+}-dependent K^+ channels (Thaler et al., 1989) because of some Ca^{2+} leakage from the vacuole during the exclusion of the micropipette.

During some experiments the light intensity was changed, and in about 50% of all cases small light-dependent changes of the cytosolic Ca^{2+} activity were observed (Fig. 1). We registered a small increase in Ca^{2+} activity of approximately 75 nM ($n = 12$) after darkening. The decrease of the cytosolic Ca^{2+} activity after illumination was smaller and less frequently registered. In most cases the light-dependent changes of the cytosolic Ca^{2+} activity were transient.

Chloride Measurements

Chloride measurements were performed in the same way as Ca^{2+} measurements, with two separate electrodes. Two distinct distributions of activities were evident, a lower activity of 2.1 mM ($-\log\{Cl^-\} = 2.68 \pm 0.03$; $n = 28$) and a higher one of about 5.9 mM ($-\log\{Cl^-\} = 2.23 \pm 0.02$; $n = 5$). During one measurement we observed a transition from the higher to the lower Cl^- activity (Fig. 5). Comparable to pH and Ca^{2+} measurements, higher Cl^- activities were observed only rarely and transitions from the high to the low activity were observed. We took this as an indication that the vacuolar Cl^- activity might be higher than the cytosolic one.

As for the other ions, we investigated the effects of light intensity changes on the intracellular Cl^- activity. When a low steady-state Cl^- activity (2.1 mM) was recorded, pronounced light-dependent changes of the Cl^- activity were observed. In contrast, no significant effect was observed during light intensity changes in the case of higher steady-state Cl^- activities (5.9 mM). A characteristic reaction of *E. viridis* to light intensity changes is shown in Figure 5. Darkening induced a transient hyperpolarization of the membrane (Köhler et al., 1983; Sauer et al., 1994). These changes in the membrane potential were too fast to be followed by the relatively slow Cl^- electrode. Therefore, the Cl^- recording showed an artifact at the beginning of each dark period. Except for this artifact, the high Cl^- activity measured at the beginning of the experiment was

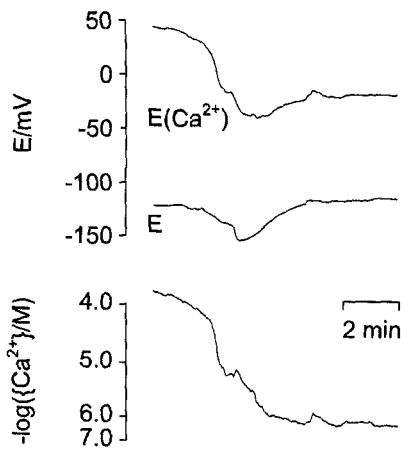

Figure 4. Transmembrane potential (E, middle trace) and intracellular Ca^{2+} activity (bottom trace) in *E. viridis*. Two electrodes were inserted into the cell, a Ca^{2+}-selective one [$E(Ca^{2+})$, upper trace] and a potential-recording one (E, middle trace). The lower trace gives the logarithmic Ca^{2+} activity. The *y* axis values were calculated from the calibration of the Ca^{2+} electrode after the experiment. A transition from a high to a low Ca^{2+} activity is shown. The low Ca^{2+} activity could not be determined reliably, since the small tip diameter of the Ca^{2+}-selective microelectrode had a decreased slope at low Ca^{2+} activities (limit of detection was 260 nM). The voltage trace shows a transient change of the electrical potential.

unaffected by the dark period. Afterward, a transition to smaller values occurred, and darkening and illumination induced pronounced changes of the Cl^- activity. A small transient hyperpolarization of the membrane was also noticeable, which coincided with the beginning of the transition of the Cl^- electrode from the higher to the lower activity. Similar transient potential changes were observed in two of five pH recordings during a transition of the electrode tip (of a double-barreled microelectrode) from the vacuole into the cytoplasm.

Cell Sap Measurements

In parallel to the measurements with ion-selective microelectrodes, we analyzed the chemical composition of the cell sap (Table I). Since 80% of the cell volume of *E. viridis* is occupied by the vacuole, the concentrations measured in the cell sap are dominated by the concentrations inside the vacuole. We assumed an activity coefficient of 0.716 corresponding to 200 mM KCl to compare concentrations measured by chemical analysis (ICP and anion chromatography) with activities measured by ion-selective microelectrodes (Table I). The K^+ and Cl^- concentrations measured directly in the cell sap were comparable to the whole-cell concentrations calculated from measurements with ion-selective microelectrodes. The Ca^{2+} concentration and the Ca^{2+} activity cannot be compared directly because most of the Ca^{2+} inside the cell is buffered. Moreover, for Ca^{2+} a much higher concentration was measured in the breakdown of dried cells (1.82 ± 0.07 mM; $n = 6$) compared to the cell sap (0.43 ± 0.02 mM; $n = 6$). Since the breakdown of complete cells includes the cell walls, the difference in the two analyses probably reflected the large amount of Ca^{2+} bound to the cell wall (Demarty et al., 1984). The most

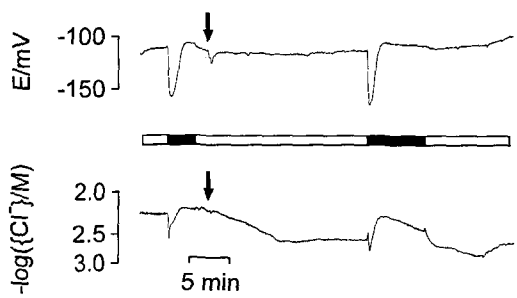

Figure 5. Transmembrane potential (E, upper trace) and intracellular Cl^- activity (lower trace) in *E. viridis*. Two electrodes were inserted into the cell, a Cl^--selective one (trace not shown) and a potential-recording one (upper trace). The lower trace gives the logarithmic Cl^- activity. The *y* axis values were calculated from the calibration of the Cl^- electrode after the experiment. After each darkening a transient hyperpolarization of the membrane was induced. The rapid downward deflections of the Cl^- trace observed in parallel with the hyperpolarizations are artifacts because the time constants of Cl^- electrodes were too high to follow the rapid membrane potential changes. At the beginning of the experiment a high Cl^- activity was recorded that was unaffected by light-dark changes. After some minutes a transition to smaller Cl^- activities occurred. The beginning of this transition (indicated by black downward pointing arrows) was accompanied by a minor transient hyperpolarization. Light-dark changes had a pronounced effect on the lower Cl^- activity.

Table I. *Comparison of cytosolic, vacuolar, and whole-cell concentrations of K^+, Ca^{2+}, and Cl^-*

Cytosolic and vacuolar concentrations were calculated from measurements with ion-selective microelectrodes, assuming an activity coefficient of 0.716. For calculations of the whole-cell concentration from ion-selective measurements, a vacuolar volume of 80% of the cell volume was assumed. The chemical composition of the cell sap was analyzed by anion chromatography (Cl^-) ICP (K^+, Ca^{2+}). Assuming a 20% probability for the K^+ electrode to impale the vacuole, we assigned the same K^+ concentration to the vacuole as to the cytoplasm, since the same K^+ activity was measured in 33 experiments (Fig. 3). The higher Cl^- concentration was attributed to the vacuole because it was observed in 15% of all measurements, thereby corresponding to the percentage of successful vacuolar impalements with H^+ and Ca^{2+} microelectrodes.

Ion	Cytoplasm	Vacuole	Whole Cell	Cell Sap
$[K^+]$/mM	182	(182)	(182)	189 ± 7 ($n = 6$)
$[Ca^{2+}]$/μM	0.162	200	160	430 ± 20 ($n = 6$)
$[Cl^-]$/mM	2.9	8.2	7.1	5.0 ± 0.2 ($n = 6$)

abundant anions in the cell sap were phosphate (29.3 ± 0.2 mM; $n = 6$) and sulfate (57.6 ± 0.7 mM; $n = 6$). The malate concentration varied strongly between two identically grown cell cultures (5.6 ± 0.3 mM, $n = 3$, and 14.2 ± 0.6 mM, $n = 3$). Nitrate was not detectable and thus had a concentration below 30 μM.

DISCUSSION

Localization of the Electrode Tips

Measurements with double-barreled, pH-selective microelectrodes are the most appropriate to determine the location of the electrode tip (Felle, 1988). Measured pH values fell into two separate pH categories of approximately 7.3 and 5.0; the two regions did not overlap. Therefore, the localization of the electrode tip could be clearly assigned either to the cytosol or to the vacuole (Fig. 2). Electrode tips of double-barreled, pH-selective microelectrodes could be inserted into the vacuole in only 12% of the experiments ($n = 68$). Tips of single-barreled, pH-selective microelectrodes were located inside the vacuole in 18% of all measurements ($n = 61$). This difference is thought to be due to differences in tip geometry. The separate potential electrodes had the same shape as the single-barreled, ion-selective electrodes. Since there is no obvious reason to explain why two identically pulled microelectrodes should have different probabilities to impale the vacuole, we concluded that tips of potential electrodes were located in the cytosol in 80% of all measurements. Despite the fact that electrodes were pushed deeply into the cells, penetration of the tonoplast was only rarely achieved. This corresponds to results of other groups working with ion-selective microelectrodes in different plant cells (Felle and Bertl, 1986a; Felle, 1993; Okazaki et al., 1994).

In some experiments an initial pH value of about 5.0 became unstable and shifted to cytosolic pH values (Fig. 2). In this case the electrode tip was excluded from the vacuole. This exclusion was not related to a movement of the pipette but was probably brought about by the tonoplast

covering the electrode tip. This may also explain why the exclusion of the pipette tip from the vacuole was a relatively slow process that took 1 to 4 min to be completed. Similar observations exist for other plant cells (Findlay and Hope, 1976; Mertz and Higinbotham, 1976; Trebacz et al., 1994). The transient change of the electrical potential frequently accompanying the exclusion of the electrode tip from the vacuole (Figs. 4 and 5) was attributed to a minor Ca^{2+} leakage from the vacuole during this process. With an increase in cytosolic Ca^{2+} activity K^+ channels in the plasma membrane were opened, thus hyperpolarizing the membrane (Thaler et al., 1989).

Electrical Potential Difference across the Tonoplast

All measurements with ion-selective microelectrodes presented here point to a common conclusion: The electrical potential difference across the tonoplast of *E. viridis* was vanishingly low. This conclusion is based on the following observations. (a) Use of θ-shaped, double-barreled and single-barreled ion-selective microelectrodes resulted in exactly the same values for the cytosolic pH, the vacuolar pH, and the intracellular K^+ activity. (b) The electrical potential measured with double-barreled, pH-selective microelectrodes in the vacuole (at pH 5.0) did not differ from the electrical potential measured in the cytoplasm. (c) The steady-state electrical potential recorded with double-barreled pH electrodes before and after the transition of the electrode tip from the vacuole into the cytosol showed no significant potential difference (Fig. 2). This last approach was probably the most direct and reliable one. Therefore, it has to be concluded that the tonoplast potential was below the error limit of our measurements, which was about ±2 mV.

A number of studies of tonoplast potentials in different plants have been conducted. Earlier examinations relied on conventional microelectrodes, assuming that electrode tips were located in the vacuole. In these works, relatively high values between −30 and −65 mV were frequently observed, but values below −10 mV were reported also (Ginsburg and Ginzburg, 1974; Lüttge and Zirke, 1974; summarized by Gibrat et al., 1985). Only when the technique of liquid-membrane ion-selective microelectrodes was applied to a variety of plant cells was it realized that the impalement of the vacuole is a rare event (Felle and Bertl, 1986a; Felle, 1993). Studies based on this technique generally reported tonoplast potentials in the range from −8 to −27 mV (Rona et al., 1982; Miller and Zhen, 1991; Zhen et al., 1991). It is interesting that a recent study reported a value as high as +50 mV (Okazaki et al., 1994).

Single-Barreled versus Double-Barreled Electrodes

Although we measured the intracellular pH and K^+ activity with both single-barreled and double-barreled microelectrodes, only single-barreled microelectrodes were used for Ca^{2+} and Cl^- measurements. It has been shown frequently that both types of electrodes yield reliable data for plant cells (Felle and Bertl, 1986a; Miller and Sanders, 1987; Felle, 1988; Miller and Zhen, 1991; Thaler et al., 1992). The important advantage of double-barreled microelectrodes is that both tips always measure in the same compartment, at the very same point of the cell, and thus always record the same electrical potential. However, in *E. viridis*, even in the rare case that one electrode is inserted into the vacuole, two separate single-barreled microelectrodes still record the same electrical potential, since the tonoplast potential is vanishingly low. Therefore, the errors that might arise in other plant cells from a different location of two electrode tips could not occur in the case of *E. viridis* (see also Thaler et al., 1992). On the other hand, double-barreled microelectrodes are difficult to fabricate and also involve a number of additional problems (Felle, 1988, 1989), and a separate variation of the tip diameter of the ion-selective electrode (Miller and Sanders, 1987) is hardly possible. Therefore, after having shown with double-barreled pH electrodes that the tonoplast potential is vanishingly low and no errors could arise from the different location of two separate electrode tips, we decided to use single-barreled microelectrodes because they are more flexible and easier to handle for our Ca^{2+} and Cl^- measurements.

Electrochemical Potential Gradients across the Tonoplast

Proton

We measured a pH gradient of 2.3 pH units across the tonoplast of *E. viridis* (Fig. 2). This corresponds to the ΔpH range reported for other plants of about 1.5 to 2.0 pH units (Taiz, 1992). Because of the low tonoplast potential, the proton motive force across the tonoplast has a chemical component that only corresponds to 13.1 kJ/mol. This serves as the energy source for all secondary active transport processes.

Potassium

With double-barreled and single-barreled K^+-selective microelectrodes, an intracellular K^+ activity of 130 mM was measured (Fig. 3). Since the electrode tips were located in the cytoplasm in about 80% of all impalements (see above), this indicated a cytosolic K^+ activity of 130 mM. This relatively high value is still in agreement with results from other plants (Flowers and Läuchli, 1983; Leigh and Wyn Jones, 1984). Although the SD of our measurements was small, the K^+ activity values, in contrast to all other ions, did not split into two groups (Fig. 3). This means that either the vacuole was never impaled, which is unlikely (n = 33), or the difference between cytosolic and vacuolar K^+ activities was very small. Cell sap analysis by ICP, which mainly reflects the vacuolar ion composition, yielded exactly the same K^+ concentration as measurements with K^+-selective microelectrodes inside the cytoplasm (Table I). This corroborated the view that the K^+ activity inside the vacuole is practically the same as in the cytoplasm. Taking into account the vanishingly small tonoplast potential, this means that K^+ was close to its equilibrium across the tonoplast. For a measurement with a K^+-selective microelectrode it follows that it is impossible to decide whether the tip of the electrode is located within the vacuole or inside the cyto-

plasm, since the electrochemical potentials for K^+ in the two compartments did not differ within the error limits.

A similar situation was recently proposed for the intracellular K^+ activity of the liverwort *Conocephalum conicum* (Trebacz et al., 1994). Some reports exist about the K^+ concentrations in the cytoplasm and the vacuole of different plants (Flowers and Läuchli, 1983; Leigh and Wyn Jones, 1984; Maathuis and Sanders, 1993) according to which the vacuolar K^+ concentration is either the same or lower than the cytosolic one, depending on the growth conditions. Only a few data sets have been published that include tonoplast potentials and K^+ gradients (Raven, 1967; Vorobiev, 1967; Rona et al., 1982). It is interesting that in three different plants the tonoplast potentials ranging from −18 to −27 mV are in each case nearly completely balanced by opposite trans-tonoplast K^+ gradients, corresponding to a +22 to +24 mV driving force. Thus, to our knowledge, all published data indicate an insignificant low electrochemical potential gradient for K^+ across the tonoplast. On this basis it is tempting to speculate that the electrical potential across the tonoplast might be determined by the K^+ concentration gradient across the tonoplast.

Light-dependent changes of the cytosolic K^+ activity in the millimolar range were reported by Felle and Bertl (1986b) in the case of the liverwort *Riccia fluitans*, whereas Trebacz et al. (1994) observed no light-dependent changes in the liverwort *C. conicum*. In *E. viridis* we did not observe light-dependent changes of the cytosolic K^+ activity, but small changes may have been obliterated by the relatively high cytosolic K^+ activity.

Calcium

The cytosolic Ca^{2+} activity of 164 nM reported here for *E. viridis* (Fig. 1) corresponds to other measurements in plant cells that range from less than 100 to 350 nM (Felle, 1989, 1993; Evans et al., 1991; Bush, 1993). This is the first value reported for a unicellular green alga. The vacuolar Ca^{2+} activity was 200 μM (Fig. 4), which is more than 1000-fold higher compared to the cytosol. The few other reported measurements of vacuolar Ca^{2+} activities are 2.3 mM in *Riccia fluitans*, 1.5 mM in *Zea mays* (Felle, 1988), and 0.3 to 1.6 mM in *Nitellopsis* (Miller and Sanders, 1987). Obviously, there is a large variability in the vacuolar Ca^{2+} activity among different plants, and *E. viridis* is at the lower end of reported values. This might be an adaptation to a natural environment of slightly acidic bog waters, in which Ca^{2+} is in very small supply. Comparison of the vacuolar Ca^{2+} activity with the Ca^{2+} concentration of the cell sap (Table I) indicates that more than 50% of the vacuolar Ca^{2+} is buffered. This buffering capacity is much smaller than the cytosolic one with which normally more than 95% of the Ca^{2+} is bound to buffering groups (Neher and Augustine, 1992). The identity of the buffering compounds inside the vacuole is not completely clear. Organic acids such as malate and citrate bind Ca^{2+} with a high affinity. Another possibility is the binding to specialized Ca^{2+}-binding proteins, which have been shown to occur in plant vacuoles (Randall, 1992). The calculated amount of Ca^{2+} bound to malate was approximately 60 μM in *E. viridis* (10 mM malate at pH 5.0). This is considerable but not sufficient, however, to explain the whole buffering capacity of the vacuole. The solubility products of the hardly soluble salts $CaHPO_4$ and $CaSO_4$ were compared with the vacuolar concentrations of the respective ions. A precipitation of these salts can be ruled out. Calcium oxalate crystals were never observed in *E. viridis*.

Light-dependent changes of the cytosolic Ca^{2+} activity were detected in 50% of all measurements. In most cases these changes were transient (Fig. 4), and the dark-induced increase of cytosolic Ca^{2+} (about 75 nM) was normally more pronounced than the light-induced decrease. This transient increase of the cytosolic Ca^{2+} activity is probably related to the transient hyperpolarization of the membrane (Fig. 5) frequently observed with *E. viridis* after darkening (Köhler et al., 1983; Sauer et al., 1994). It was shown that this transient hyperpolarization is due to the transient opening of Ca^{2+}-dependent K^+ channels in the plasma membrane (Thaler et al., 1989). Trebacz et al. (1994) could not detect any light-dependent changes of the cytosolic Ca^{2+} activity in the liverwort *C. conicum* , whereas there was an obvious increase of cytosolic Ca^{2+} during action potentials. With the same method, using ion-selective microelectrodes, Miller and Sanders (1987) found strong light-induced changes of the cytosolic Ca^{2+} activity in the *Nitellopsis*. A 6- to 7-fold permanent decline was observed during intense illumination, and it was proposed that this depletion of cytosolic free Ca^{2+} constitutes a fundamental signal that enables the rate of extrachloroplastic metabolism to be geared to photosynthetic processes in the chloroplast (Miller and Sanders, 1987). This does not seem to hold for green plant cells in general since light-dependent changes of the cytosolic Ca^{2+} activity are markedly different in various plant cells.

Chloride

Measurements with Cl^--selective microelectrodes yielded two distributions of activities, a lower one of about 2.1 mM and a higher one of about 5.9 mM (Table I). We assigned the lower activity to the cytoplasm and the higher one to the vacuole for the following reasons. (a) Only 15% of the measurements showed activities of about 5.9 mM, and as discussed above, this corresponded to the probability of impaling the vacuole. (b) We observed transitions from the high to the low activity (Fig. 5) (but never the other way around), probably caused by an exclusion of the electrode tip from the vacuole. (c) Light-dependent changes of the Cl^- activity were measured only at lower steady-state activities (Fig. 5), and these changes were attributed to Cl^- fluxes across the chloroplast envelope (Thaler et al., 1992). (d) Measurements of the Cl^- concentration in the cell sap by anion chromatography confirmed the higher Cl^- concentration inside the vacuole (Table I). Our measurements thus indicated a Cl^- activity of 2.1 mM for the cytosol and 5.9 mM for the vacuole.

A general problem with the application of Cl^--selective microelectrodes is the low discrimination among different organic and inorganic anions (Kondo et al., 1989). NO_3^- is

especially preferred 5- to 15-fold (Kondo et al., 1989; Trebacz et al., 1994) by the Cl^--selective microelectrodes used here (Fluka No. 24902). Taking into account the anion composition of the cell sap as measured by anion chromatography (with $[NO_3^-] = 30$ μM) and based on the published selectivity coefficients (Kondo et al., 1989), we overestimated the Cl^- activity, as measured by Cl^--selective microelectrodes, by 0.8 mM at worst. This may explain the deviation between the Cl^- concentration measured in the cell sap and the whole-cell concentration calculated from Cl^- activities measured in the cytoplasm and in the vacuole (Table I). In any case, our data clearly showed a Cl^- concentration gradient across the tonoplast. The equilibrium potential of this gradient was larger than −20 mV. A tonoplast potential of this magnitude would have been easily detected in *E. viridis* but was absent here. A tonoplast potential close to 0 mV and a remarkable anion gradient across the tonoplast at the same time are in obvious contrast to the common assumption (Blumwald and Poole, 1985; Hedrich et al., 1988; Martinoia, 1992; Taiz, 1992) that the tonoplast potential is responsible for the accumulation of anions inside the vacuole. Until now, direct measurements of the cytosolic and vacuolar Cl^- activity by means of ion-selective microelectrodes were only performed for one plant species other than *E. viridis*. In *C. conicum* a 5- to 6-fold concentration gradient for Cl^- across the tonoplast was measured. Although not measured directly, there were some indications that the tonoplast potential was negligible (Trebacz et al., 1994). Measurements with NO_3^--selective microelectrodes were performed in *Chara* and in barley roots (Miller and Zhen, 1991; Zhen et al., 1991). Despite the high accumulation of NO_3^- inside the vacuole in both plants, the measured tonoplast potential was low. Active transport of Cl^- is believed to occur at the tonoplast of *Chara* (MacRobbie, 1970). There is some experimental evidence for H^+-coupled Cl^- and NO_3^- transport in tonoplast vesicles (Blumwald and Poole, 1985; Schumaker and Sze, 1987b). Therefore, we conclude that Cl^- transport into the vacuole is not accomplished by the tonoplast potential via anion channels. Instead, Cl^- uptake into the vacuole is an active process probably involving a Cl^-/H^+ antiporter.

We observed significant light-dependent changes of the Cl^- activity in the cytoplasm but not in the vacuole (Fig. 5). Thaler et al. (1992) showed that the light-dependent H^+ and Cl^- activity changes in the cytoplasm are caused by light-driven H^+ and Cl^- uptake across the chloroplast envelope into the thylakoid lumen. There are probably no corresponding light-dependent H^+ and Cl^- fluxes across the tonoplast, since neither the pH nor the Cl^- activity inside the vacuole changed significantly upon illumination or darkening.

CONCLUSIONS

The electrochemical potential gradients for H^+, K^+, Ca^{2+}, and Cl^- across the tonoplast of *E. viridis* are depicted in Figure 6. The electrical potential difference across the tonoplast was negligibly small. As in other plant cells, there were considerable driving forces for H^+ and Ca^{2+} in the direction of the cytoplasm, the Ca^{2+} gradient being slightly larger than the pH gradient. There were no obvious light-dependent changes of the cytosolic Ca^{2+} activity. Approximately 60% of the vacuolar Ca^{2+} was bound to buffering groups. K^+ was in equilibrium across the tonoplast. Cl^- accumulated inside the vacuole in the absence of a significant tonoplast potential. It is proposed that the tonoplast potential is determined by the K^+ concentration gradient and that Cl^- actively accumulates inside the vacuole by a proton-coupled transport.

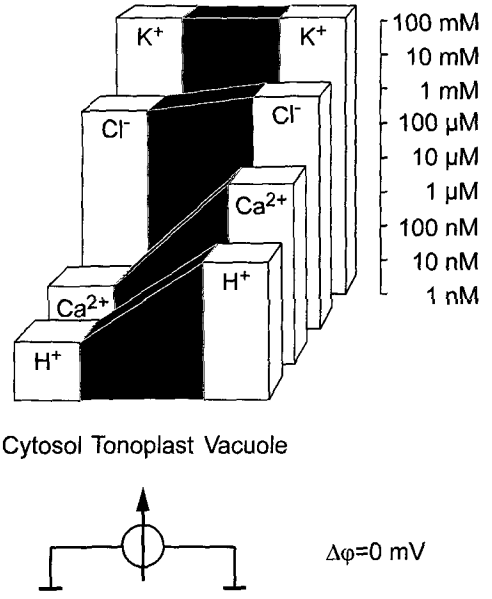

Figure 6. Schematic presentation of the electrochemical potential gradients of H^+, K^+, Ca^{2+}, and Cl^- across the tonoplast (in black) of *E. viridis*. Ion activities are given by the heights of the columns on a logarithmic scale. Differences in height directly reflect the chemical gradients, which are also indicated by the steepness of the black intermediary area. At the bottom a trans-tonoplast electrical potential ($\Delta\varphi$) close to 0 mV is indicated. For lucidity error bars have been omitted. For the exact values (means ± SE) see text.

ACKNOWLEDGMENTS

We would like to thank Dr. W.M. Kaiser for analyses by anion chromatography, Mrs. F. Reisberg for analyses by ICP, and Dr. I.I. Pottosin for the helpful discussions.

Received May 18, 1995; accepted September 5, 1995.

LITERATURE CITED

Alexandre J, Lassalles JP, Kado RT (1990) Opening of Ca^{2+} channels in isolated red beet vacuole membranes by inositol 1,4,5-trisphosphate. Nature **343:** 567–570

Ammann D (1986) Ion-selective microelectrodes. Principles, Design and Application. Springer-Verlag, New York

Ammann D, Bührer T, Schefer U, Müller M, Simon W (1987) Intracellular neutral carrier-based Ca^{2+} microelectrode with subnanomolar detection limit. Pflugers Arch Eur J Physiol **409:** 223–228

Bertl A, Blumwald E, Coronado R, Eisenberg R, Findlay GP, Gradmann D, Hille B, Köhler K, Kolb H-A, MacRobbie EAC, Meissner G, Miller C, Neher E, Palade P, Pantoja O, Sanders

D, Schroeder JI, Slayman C, Spanswick R, Walker A, Williams A (1992) Electrical measurements on endomembranes. Science **258:** 873–874

Blumwald E, Poole RJ (1985) Nitrate storage and retrieval in *Beta vulgaris*: effects of nitrate and chloride on proton gradients in tonoplast vesicles. Proc Natl Acad Sci USA **82:** 3683–3687

Bush DS (1993) Regulation of cytosolic calcium in plants. Plant Physiol **103:** 7–13

Demarty M, Morvan C, Thellier M (1984) Calcium and the cell wall. Plant Cell Environ **7:** 441–448

Evans DE, Briars S-A, Williams LE (1991) Active calcium transport by plant cell membranes. J Exp Bot **42:** 285–303

Felle H (1988) Cytoplasmic free calcium in *Riccia fluitans* L. and *Zea mays* L.: interaction of Ca^{2+} and pH? Planta **176:** 248–255

Felle H (1989) Ca^{2+}-selective microelectrodes and their application to plant cells and tissues. Plant Physiol **91:** 1239–1242

Felle H, Bertl A (1986a) The fabrication of H^+-selective microelectrodes for use in plant cells. J Exp Bot **37:** 1416–1428

Felle H, Bertl A (1986b) Light-induced cytoplasmic pH changes and their interrelation to the activity of the electrogenic proton pump in *Riccia fluitans*. Biochim Biophys Acta **848:** 176–182

Felle HH (1993) Ion-selective microelectrodes: their use and importance in modern plant cell biology. Bot Acta **106:** 5–12

Findlay GP, Hope AB (1976) Electrical properties of plant cells: methods and findings. *In* U Lüttge, MG Pitman, ed, Encyclopedia of Plant Physiology, New Series, Vol 2A. Springer-Verlag, New York, pp 53–92

Flowers TJ, Läuchli A (1983) Sodium versus potassium: substitution and compartmentation. *In* A Läuchli, RL Bieleski, eds, Encyclopedia of Plant Physiology, New Series, Vol 15B. Springer-Verlag, New York, pp 652–681

Fry CH, Hall SK, Blatter LA, McGuigan JAS (1990) Analysis and presentation of intracellular measurements obtained with ion-selective microelectrodes. Exp Physiol **75:** 187–198

Gavin O, Pilet P-E, Chanson A (1993) Tonoplast localization of a calmodulin-stimulated Ca^{2+}-pump from maize roots. Plant Sci **92:** 143–150

Gibrat R, Barbier-Brygoo H, Guern J, Grignon C (1985) Transtonoplast potential difference and surface potential of isolated vacuoles. *In* B Marin, ed, Biochemistry and Function of Vacuolar Adenosine-Triphosphatase in Fungi and Plants. Springer-Verlag, Berlin, pp 83–97

Ginsburg H, Ginzburg BZ (1974) Radial water and solute flows in roots of *Zea mays*. IV. Electrical potential profiles across the root. J Exp Bot **25:** 28–35

Hedrich R, Barbier-Brygoo H, Felle H, Flügge U-I, Lüttge U, Maathuis FJM, Marx S, Prins HBA, Raschke K, Schnabl H, Schroeder JI, Struve I, Taiz L, Ziegler P (1988) General mechanisms for solute transport across the tonoplast of plant vacuoles: a patch-clamp survey of ion channels and proton pumps. Bot Acta **101:** 7–13

International Union of Pure and Applied Chemistry (1976) Recommendations for nomenclature of ion-selective electrodes. Pure Appl Chem **48:** 129–132

Köhler K, Geisweid H-J, Simonis W, Urbach W (1983) Changes in membrane potential and resistance caused by transient increase of potassium conductance in the unicellular green alga *Eremosphaera viridis*. Planta **159:** 165–171

Kondo Y, Bührer T, Seiler K, Frömter E, Simon W (1989) A new double-barrelled, ionophore-based microelectrode for chloride ions. Pflugers Arch Eur J Physiol **414:** 663–668

Leigh RA, Wyn Jones RG (1984) A hypothesis relating critical potassium concentrations for growth to the distribution and functions of this ion in the plant cell. New Phytol **97:** 1–13

Lüttge U, Zirke G (1974) Attempts to measure plasmalemma and tonoplast electropotentials in small cells of the moss *Mnium* using centrifugation techniques. J Membr Biol **18:** 305–314

Maathuis FJM, Sanders D (1993) Energization of potassium uptake in *Arabidopsis thaliana*. Planta **191:** 302–307

MacRobbie EAC (1970) The active transport of ions in plant cells. Q Rev Biophys **3:** 251–294

Martinoia E (1992) Transport processes in vacuoles of higher plants. Bot Acta **105:** 232–245

Meier PC, Ammann D, Morf WE, Simon W (1980) Liquid-membrane ion-selective electrodes and their biomedical applications. *In* J Koryta, ed, Medical and Biological Applications of Electrochemical Devices. John Wiley & Sons, New York, pp 13–91

Mertz SM Jr, Higinbotham N (1976) Transmembrane electropotential in barley roots as related to cell type, cell location, and cutting and aging effects. Plant Physiol **57:** 123–128

Miller AJ, Sanders D (1987) Depletion of cytosolic free calcium induced by photosynthesis. Nature **326:** 397–400

Miller AJ, Zhen R-G (1991) Measurement of intracellular nitrate concentrations in *Chara* using nitrate-selective microelectrodes. Planta **184:** 47–52

Neher E, Augustine GJ (1992) Calcium gradients and buffers in bovine chromaffin cells. J Physiol **450:** 273–301

Okazaki Y, Tazawa M, Iwasaki N (1994) Light-induced changes in cytosolic pH in leaf cells of *Egeria densa*: measurements with pH-sensitive microelectrodes. Plant Cell Physiol **35:** 943–950

Pfeiffer W, Hager A (1993) A Ca^{2+}-ATPase and a Mg^{2+}/H^+-antiporter are present on tonoplast membranes from roots of *Zea mays* L. Planta **191:** 377–385

Randall SK (1992) Characterization of vacuolar calcium-binding proteins. Plant Physiol **100:** 859–867

Raven JA (1967) Ion transport in *Hydrodictyon africanum*. J Gen Physiol **50:** 1607–1625

Rea PA, Sanders D (1987) Tonoplast energization: two H^+ pumps, one membrane. Physiol Plant **71:** 131–141

Rona J-P, Cornel D, Grignon C, Heller R (1982) The electrical potential difference across the tonoplast of *Acer pseudoplatanus* cells. Physiol Veg **20:** 459–463

Sauer G, Simonis W, Schönknecht G (1994) Divalent cation and anion currents are activated during the dark-induced transient hyperpolarization of the plasma membrane of the green alga *Eremosphaera viridis*. J Exp Bot **45:** 1403–1412

Schröppel-Meier G, Kaiser WM (1988) Ion homeostasis in chloroplasts under salinity and mineral deficiency. I. Solute concentrations in leaves and chloroplasts from spinach plants under NaCl or $NaNO_3$ salinity. Plant Physiol **87:** 822–827

Schumaker KS, Sze H (1985) A Ca^{2+}/H^+ antiport system driven by the proton electrochemical gradient of a tonoplast H^+-ATPase from oat roots. Plant Physiol **79:** 1111–1117

Schumaker KS, Sze H (1987a) Inositol 1,4,5-trisphosphate releases Ca^{2+} from vacuolar membrane vesicles of oat roots. J Biol Chem **262:** 3944–3946

Schumaker KS, Sze H (1987b) Decrease of pH-gradients in tonoplast vesicles by NO_3^- and Cl^-: evidence for H^+-coupled anion transport. Plant Physiol **83:** 490–496

Taiz L (1992) The plant vacuole. J Exp Biol **172:** 113–122

Thaler M, Simonis W, Schönknecht G (1992) Light-dependent changes of the cytoplasmic H^+ and Cl^- activity in the green alga *Eremosphaera viridis*. Plant Physiol **99:** 103–110

Thaler M, Steigner W, Förster B, Köhler K, Simonis W, Urbach W (1989) Calcium activation of potassium channels in the plasmalemma of *Eremosphaera viridis*. J Exp Bot **40:** 1195–1203

Trebacz K, Simonis W, Schönknecht G (1994) Cytoplasmic Ca^{2+}, K^+, Cl^-, and NO_3^- activities in the liverwort *Conocephalum conicum* L. at rest and during action potentials. Plant Physiol **106:** 1073–1084

Tsien RY, Rink TJ (1980) Neutral carrier ion-selective microelectrodes for measurement of intracellular free calcium. Biochim Biophys Acta **599:** 623–638

Tyerman SD (1992) Anion channels in plants. Annu Rev Plant Physiol Plant Mol Biol **43:** 351–373

Vorobiev LN (1967) Potassium ion activity in the cytoplasm and the vacuole of cells of *Chara* and *Griffithsia*. Nature **216:** 1325–1327

Zhen R-G, Koyro HW, Leigh RA, Tomos AD, Miller AJ (1991) Compartmental nitrate concentrations in barley root cells measured with nitrate-selective microelectrodes and by single-cell sap sampling. Planta **185:** 356–361